Low-Lying Spin States of Iron(II) Porphine

Pawel M. Kozlowski and Thomas G. Spiro*

Department of Chemistry, Princeton University, Princeton, New Jersey 08544

Attila Bérces and Marek Z. Zgierski

Steacie Institute for Molecular Science, National Research Council of Canada, Ottawa, Ontario, Canada K1A OR6

Received: October 15, 1997

Geometries and force-fields of the low-lying spin states of iron(II) porphine are calulated with nonlocal density functional methods. The ground state is identified as the $^3A_{2g}$ state. It is shown that the Fe atom is in the porphine plane for all spin states, but that the high-spin state potential surface intersects the triplet-state potential surfaces along the doming-mode coordinate when the iron atom is displaced about 0.4 Å from the NNNN plane. This intersection is the result of an electron occupying the antibonding $d_{x^2-y^2}$ orbital in the quintet states. The doming mode of the porphine is predicted to be at 71 cm^{-1}, close to the 75 cm^{-1} frequency determined from coherent reaction dynamics in myoglobin.

1. Introduction

Iron porphyrins continue to be the subject of active experimental and theoretical research because they serve as structural models for the active sites of heme proteins.[1] The d^6 iron(II) ion can exhibit three spin states: $S = 0$ (low-spin), $S = 1$ (intermediate-spin), and $S = 2$ (high-spin). The ground state depends on the relative energies of the iron d orbitals, which in turn depend on the ligand field of the porphyrin and of the axial ligands, if any. These fields determine important structural parameters, including porphyrin planarity and core size and the displacement of the iron atom with respect to the mean porphyrin plane. Elucidation of the spin-state/stereochemical relationship in iron(II) porphyrins has important consequences for understanding how hemoproteins perform their biological functions.[2] Knowledge of the force field is important for correlating spectroscopic observations with structural data. For example, Mössbauer spectroscopy[3] on deoxymyoglobin, with a five-coordinate heme site, indicates that, at low temperatures, the iron motion follows a harmonic oscillation, but, above 165 K, the motion becomes anharmonic, with a rapid increase of mean amplitude. A simple model consisting of two closely lying states of different spin undergoing an avoided crossing owing to spin−orbit interaction was proposed to explain these experimental findings.[4] It was essential for this model that the frequency of the doming mode is very different in the two states, and that the two states have different equilibrium positions of the iron atom with respect to the plane of the four nitrogen atoms. However, different conformational states of the protein are also expected to contribute to the iron-atom dynamics, modifying the parameters of a simple two-state model.[4,5] To get a better understanding of iron-atom motion, reliable force fields of iron(II) porphyrins in various spin states are required.

In this paper we focus on the simplest iron(II) porphyrin, Fe(II)P (P = porphine), with D_{4h} symmetry (see Figure 1). It is generally accepted that the ground state has intermediate spin, although which electronic configuration has the triplet ground state remains controversial. There are four possible intermediate spin states:

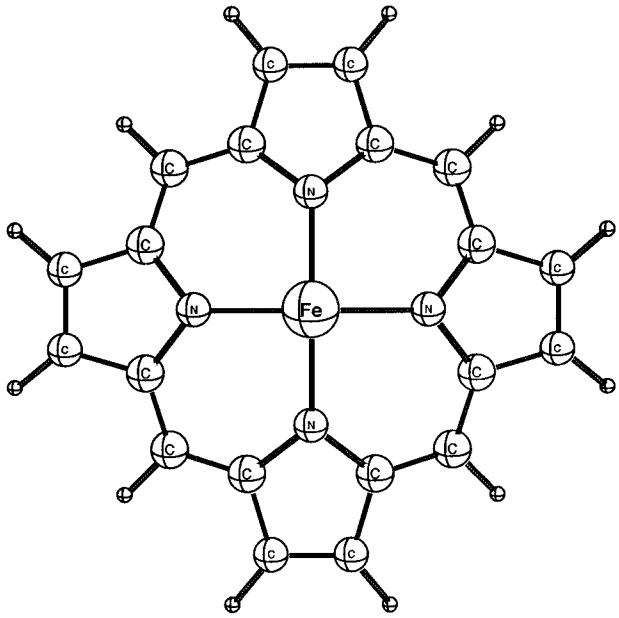

Figure 1. Reference structure of iron porphine.

$^3A_{2g}(d_{xy})^2(d_{xz}, d_{yz})^2(d_{z^2})^2$, $^3B_{2g}(d_{xy})^1(d_{xz}, d_{yz})^4(d_{z^2})^1$, $^3E_g(A)(d_{xy})^2(d_{yz}, d_{xz})^3(d_{z^2})^1$, and $^3E_g(B)(d_{xy})^1(d_{yz}, d_{xz})^3(d_{z^2})^2$

but states of $^3B_{2g}$ and ^3E_g (A) symmetry are at high energies, and the $^3B_{2g}$ spin state is incompatible with Mössbauer[6] and NMR[7] data. The proton NMR data for iron(II) tetraphenyloporphyrin, Fe(II)(TPP), shows large π contact shifts, indicating that the orbital ground state is nondegenerate.[7] This leads to the conclusion that the ground state has an $^3A_{2g}$ configuration, a prediction that is consistent with magnetic data[6] and Mössbauer spectra of Fe(II)(TPP).[8] Mössbauer spectroscopy provides the most detailed information on the ground-state orbital configuration,[9] the isomer shift and quadrupole splitting being directly related to structural details of the iron atom. On the other hand, the resonance Raman spectrum of iron(II) octa-

S1089-5647(97)03346-4 CCC: $15.00
Published on Web 03/17/1998

TABLE 1: Low-Lying Electronic States of Iron(II) Porphyrin

	configuration					ΔE^a									
state	x^2-y^2	z^2	xy	yz	xz	SCF[b]	SCF[c]	CI[c]	CI[d]	CI[e]	LDF[f]	MDCP[g,h]	LDA[i]	NLDA[i]	B3LYP[j]
$^5A_{1g}$	1	2	1	1	1	−1.53	−1.40	−0.10		0.28	1.44	0.64	1.10	0.59	0.03
^5E_g	1	1	1	1.5	1.5	−1.30	−1.19	−0.83		0.39	1.74		1.08	0.69	0.27
$^5B_{2g}$	1	1	2	1	1	−1.18	−1.05	0.09		0.63	1.18		1.33	0.87	0.50
$^3A_{2g}$	0	2	2	1	1	−0.32	−0.29	0.47	−0.27	−0.03	0.25	0.00	0.06	−0.08	−0.27
^3E_g (A)	0	1	2	1.5	1.5	0.00	0.00	0.00	0.00	0.00	0.00		0.00	0.00	0.00
$^3B_{2g}$	0	1	1	2	2	0.56	0.51	0.20		0.39	0.53		0.32	0.14	0.35
^3E_g (B)	0	2	1	1.5	1.5	1.43	1.42	1.12		1.03	0.88				0.65
$^1A_{1g}$	0	0	2	2	2	1.39	1.36	1.06		0.98	1.20		1.35	1.28	1.34
$^1A_{1g}$	0	2	0	2	2		5.89				3.67				
	0	2	2	1	1							0.55			

[a] Energies in eV with respect to the ^3E_g (A) state as reference. [b] From Obara and Kashiwagi.[28] [c] From Rawlings, Gouterman, Davidson, and Feller.[30] [d] From Rohmer.[31] [e] From Edwards, Weiner, and Zerner.[32] [f] From Delley.[33] [g] Molecular dynamics method of Carr and Parrinello (MDCP).[35] [h] Energies with respect to the $^3A_{2g}$ state without orbital symmetry restrictions.[36] [i] Present work, local and nonlocal DFT calculations performed with the ADF program.[21,22] [j] Present work, nonlocal DFT with the B3-LYP functional.[16,17]

ethyloporphyrin has been interpreted in terms of a $^3E(A)_g$ ground state,[10] but the vibrational frequencies are mainly a function of the occupancy of the $d_{x^2-y^2}$ orbital and do not rule out a $^3A_{2g}$ ground state.

Ab initio electronic structure calculations for Fe(II)P represent a challenging problem because accurate energies require the use of correlated wave functions. Hartree−Fock (HF) theory is generally inadequate for transition-metal systems and metalloporphyrins and also fails to give realistic geometries of the porphyrin macrocyclic ring;[11,12] instead of bond equalization, a broken-symmetry resonance structure is predicted.[11,13,14] More advanced methods, including configuration interaction (CI) and local density functional theory, still fail to predict the ground state of Fe(II)P, as discussed in the next section.

The aim of this study is to reliably investigate the ground state and several low-lying excited states of four-coordinate Fe(II)P. Within these states optimized geometries and force fields are calculated by nonlocal density functional methods. We investigate the nature of the iron out-of-plane displacement forces on the analysis of normal modes having large amplitude motion of the iron atom.

2. Electronic Energies

Density Functional Theory (DFT) has become the method of choice for the quantum-chemical calculation of molecular potential surfaces because it accounts for the correlation energy in a computationally efficient manner. DFT-predicted geometries have been found to agree well with experiment, while DFT force fields, when properly scaled, reproduce experimental frequencies better than other methods. The successful calculation of the vibrational spectra of free base porphine,[13] and of magnesium and zinc metalloporphyrins,[14] and the recent comprehensive study of the inner hydrogen migration in free base porphine,[15] lend confidence in applying DFT to Fe(II)P.

Most of the analysis in this study is based on nonlocal DFT with the B3-LYP[16,17] exchange-correlation functional as implemented in the Gaussian 94 suite of programs,[18] using the 6-31G(d) basis set for H, C, and N and the VTZ basis of Ahlrichs[19] for Fe. To compare results with alternative DFT approaches, we carried out geometry optimizations using the Amsterdam density functional (ADF) program (version 2.0.1). The ADF program is derived from the work of Baerends et al.[20] and was developed at the Free University of Amsterdam[21] and at the University of Calgary.[22] The atomic orbitals on iron were described by an uncontracted triple-ζ STO basis set,[23] while a double-ζ STO basis set was used for C, N, and H, augmented by single-ζ polarization functions. The $1s^2$ configuration of carbon and nitrogen and the $1s^22s^22p^6$ configuration of iron were assigned to the core and treated by the frozen-core approximation. A set of auxiliary s, p, d, f, g, and h STO functions, centered on all nuclei, was used in order to fit the molecular density and represent the Coulomb and exchange potentials accurately in each SCF cycle.[24] We applied the local density approximation (LDA)[25] in the first set of calculations, and we also included the gradient corrections of Becke and Perdew to the exchange and correlation potentials[26] in the second set (BP).

Several low-lying electronic states of planar Fe(II)P were analyzed with the B3-LYP functional. Previous electronic structure calculations of Fe(II)P have been restricted to single-point energy calculations using the same geometry for different spin states, usually taken from X-ray structures of similar compound.[27−34] In our study, full geometry optimization was undertaken of all electronic states, and all stationary points were subjected to vibrational analysis using analytical second derivatives. Since the objective was to characterize electronic states of planar Fe(II)P, D_{4h} symmetry constraints were applied, except for the E states, for which the effective symmetry was lowered to D_{2h}, in order to take account of Jahn−Teller distortion along b_{1g} and b_{2g} coordinates. The results of our calculations are summarized in Table 1, where they are compared with previous calculations. Two early SCF calculations[28,30] gave a high-spin ground state, contrary to experimental findings. This error can be attributed to the HF method, which exaggerates the ionic character of the wave function and underestimates the bonding between the metal and ligand. The inclusion of correlation energy,[30−32] which diminished the exchange effect, raised the quintet energies, and the calculation by Edwards et al.[32] correctly predicted $^3A_{2g}$ as the ground state, although it was only 0.03 eV below ^3E_g(A). This gap increased somewhat in the more extensive CI calculations by Rohmer.[31] The small energy difference between $^3A_{2g}$ and ^3E_g(A) makes the ordering sensitive to the details of the calculations. The local DFT calculations of Delley[33] (column marked LDF in Table 1) placed ^3E_g(A) lower, by 0.25 eV, while our local density calculations (column marked LDA) lowered the gap to 0.06 eV, probably owing to geometry optimization. In recent calculations Parrinello and co-workers[35] used the molecular dynamics method of Carr and Parrinello (column marked MDCP) to investigate electronic states of FeP. Their lowest triplet, obtained without the restriction of the spatial symmetry of the orbitals, had a d orbital occupation similar to the $^3A_{2g}$ state. Their lowest singlet had the iron d_{z^2} orbital doubly occupied, while d_{yz} and d_{xz} orbitals were singly occupied. This open-shell singlet was energetically

TABLE 2: Comparison of the Core Sizes for Different Spin States of Iron(II) Porphyrin Based on DFT Calculations

electronic state	core size in Å	exp.	system
$^1A_{1g}$	2.002	2.004	Fe(II)(TPP)(Pip)$_2$ [b]
$^3A_{2g}$	2.001	1.972	Fe(II)(TPP)[c]
$^3E(A)$	2.002 [1.999][a]		
$^3B_{2g}$	2.000		
$^3E(B)$	2.012 [2.011]		
$^5A_{1g}$	2.061	2.057	Fe(II)(TPP)(THF)$_2$ [d]
^5E_g	2.053 [2.070]		
$^5B_{2g}$	2.061		

[a] Core sizes correspond to the Fe−N distance in ideal D_{4h} symmetry, except for E states where the lower symmetry (D_{2h}) reflects the Jahn−Teller distortion (x [y] denotes the core size in x- and y-directions). [b] TPP = tetraphenyloporphine, Pip = piperidine.[37] [c] Reference 6. [d] THF = tetrahydrofuran.[38]

closer to the lowest triplet than the lowest quintet. Our calculations with nonlocal DFT place $^3A_{2g}$ lowest, by 0.08 eV for the ADF (column marked NLDA) and by 0.27 eV for the B3-LYP functional, which we adopted for rest of our calculations. Interestingly, B3-LYP raises the exchange effect and lowers the quintet energies close to the triplet energies. $^5A_{1g}$ is now only 0.30 eV above $^3A_{2g}$ and is essentially degenerate with $^3E_g(A)$.

An important issue is the relationship between electronic state and the size of the porphyrin core containing the Fe. Our geometry-optimized B3-LYP results are given in Table 2. There is excellent agreement between the core sizes calculated for singlet and quintet states and the X-ray crystal structures for low-spin and high-spin six-coordinate Fe(II) porphyrins[37,38] Since there are no axial ligands in our calculations, the good agreement with experiment implies that the length of the metal−N (porphyrin) bonds is determined mainly by the electronic state and specifically the occupancy of the antibonding $d_{x^2-y^2}$ orbital, as has usually been assumed. The influence of 1−3 nonbonding interaction between the axial ligand atom and the porphyrin N atoms appears to be of secondary importance. Consistent with a decisive role for the $d_{x^2-y^2}$ orbital, the calculated core size is as small for the triplet states as for the singlet state. The experimental core size is actually smaller than calculated for the four-coordinate triplet Fe(II)P. This discrepancy is readilly explained by the out-of-plane ruffling of the porphyrin ring observed in the Fe(II)TPP crystal structure.[6] This distortion is known to shorten metal−N (porphyrin) bonds, as in the case of NiOEP.[39] In our calculation the porphine was constrained to be planar, and the minimum core size for a planar porphyrin appears to be 2.00 Å, as deduced experimentally by Hoard long ago.[40] Had the planar porphyrin structure been exposed to crystal-packing forces, the predicted core size would no doubt have decreased, as is observed experimentally.

3. Out-of-Plane Displacement

Since the coupling between the electronic state and displacement of the iron atom from the porphyrin plane is a central aspect of heme protein dynamics, we calculated the dependence of the electronic energies as a function of this displacement, using the B3-LYP functional. The iron was moved out of the plane in 0.05 Å increments, and the nitrogen atoms were allowed to follow by tilting the pyrrole rings about the $C_\alpha-C_\alpha$ axis. The structure was then reoptimized with fixed Fe distance to the plane of the four nitrogens. For all states, the energy is lowest when the iron is in the plane. We found that promoting an electron to the $d_{x^2-y^2}$ orbital to produce a quintet state does

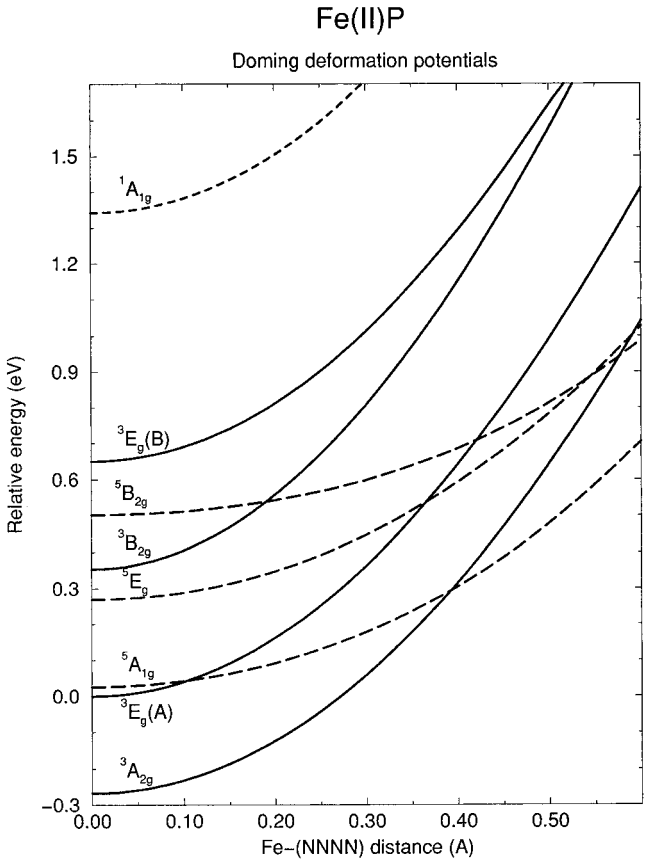

Figure 2. Potential energy curves calculated as a function of the out-of-plane displacement of the iron atom for low-, intermediate-, and high-spin states.

not in itself force the Fe out of the porphine plane, as has been sometimes suggested,[41,42] and interestingly predicted recently by Rovira et al.[35] using the molecular dynamics method of Carr and Parrinello. Instead the antibonding interaction results in porphine core expansion, as discussed above (see also refs 41−43 for detailed discussion). However, the energy increases much less rapidly with Fe displacement for the quintet states than for the singlet or triplet state (Figure 2). The flatter potential curve for the quintet state reflects the tradeoff between decreased bonding and decreased antibonding interactions as the Fe moves away from the porphine nitrogen atoms. The antibonding interaction is absent for the triplet and singlet states, in which the $d_{x^2-y^2}$ orbital is empty, and their sharper potential curves reflect only the decreased bonding with increasing Fe displacement.

Because of its flat potential curve, the $^5A_{1g}$ state becomes the ground state for Fe displacements greater than 0.4 Å. In deoxyhemoglobin (Hb) and myoglobin (Mb), the out-of-plane distance is ∼0.5 Å, accounting for their high-spin ground state. However, the potential curves in Figure 2 establish that the high-spin configuration does not by itself require the Fe displacement. Rather the out-of-plane structure must be stabilized by the axial ligand, which is the imidazole side chain of the proximal histidine residue.

To investigate this matter further we carried out energy minimization at the B3-LYP level on a five-coordinate Fe(II)P complex. To avoid expensive computational effort we simplified the ligand to NH_2 mimicking imidazole and used C_{2v} symmetry constrains for the optimization. An electron was added (NH_2^-) or subtracted (NH_2^+) in order to produce a closed electronic shell on N. Both ligands produced an out-of-plane optimized structure with the Fe displacement 0.18 Å (NH_2+)

TABLE 3: Scaling Factors Used in the Scaled Quantum Mechanical Force Field[a]

coordinate type	scale factor
C−N, C−C, or Fe−N stretches	0.9337
C−H stretches	0.9122
ring symmetrized deformations	0.9880
ring symmetrized torsions	0.9619
CH in plane rockings	0.9340
out-of-plane modes	0.9486

[a] Scaling factors optimized on free base porphyrine and its isotopomers.[13]

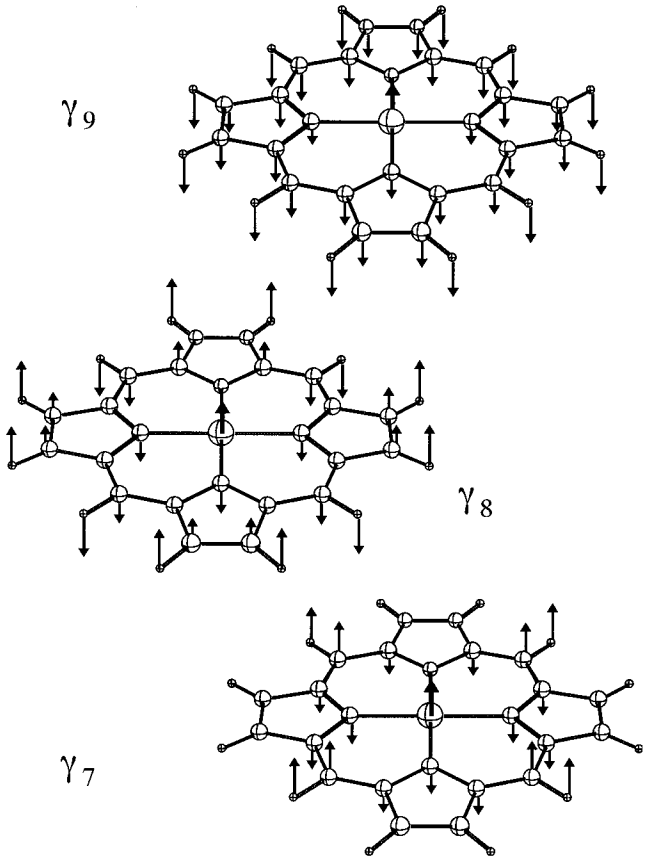

Figure 3. Eigenvectors of the γ_9, γ_8, and γ_7 out-of-plane vibrations of iron porphyrin.

or 0.19 Å (NH_2^-) from the mean porphine plane. This displacament is smaller than reported for deoxy Hb or Mb but is in good agreement with the 0.2 Å reported for model compounds.[2] The displacement increases to 0.4 Å when 2-methyloimidazole is used as an axial ligand in the model compounds Fe(TPP)(2-MeIm) and Fe(TpivPP)(2-MeIm).[48] The 2-methyl group sterically hinders movement of the Fe toward the porphyrin plane and has been used as a functional mimic of the low-affinity T state of Hb. We infer that in deoxy Hb and Mb, protein forces likewise increase the Fe displacement to 0.5 Å, from the 0.2 Å optimal distance.

4. Vibrational Displacements of the Iron

To determine the frequency of vibrations involving significant Fe motion, we evaluated the force field for each spin state at the B3-LYP level, transformed it to a set of nonredundant natural internal coordinates,[13] and scaled the force constants according to the formula $F'_{ij} = (\lambda_i\lambda_j)^{1/2} F_{ij}$, with a set of six scaling factors which had previously been optimized for free base porphine,[13] and tested for magnesium and zinc metalloporphyrins.[14] The

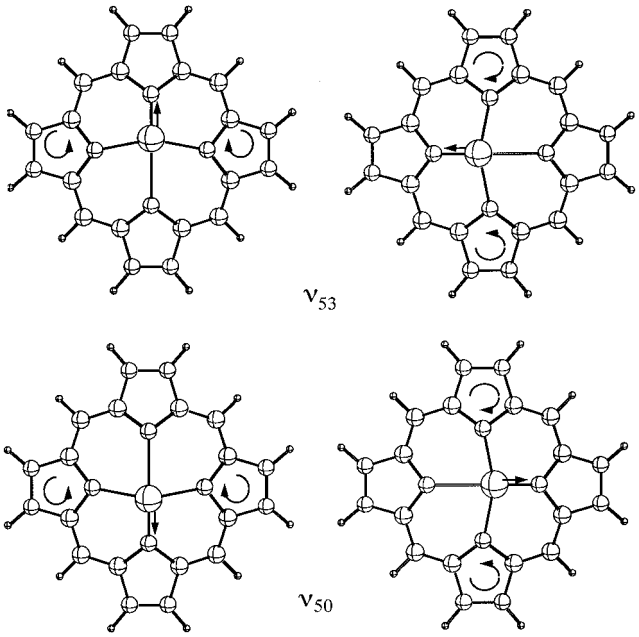

Figure 4. Eigenvectors of the ν_{53} and ν_{50} in-plane vibrations of iron porphyrin.

numerical values are given in Table 3. For planar Fe(II)P, we found seven vibrational modes whose eigenvectors show significant displacement of Fe (Figures 3 and 4). Since the Fe is at the center of symmetry, these are all IR-active, a_{2u} and e_u, and Raman-inactive. Four of these are pairs of e_u modes: ν_{50} and ν_{53} (the mode labeling scheme has been worked out for NiOEP, ref 52). They involve a mixture of $Fe-N_{pyrrole}$ stretching and pyrrole rotation coordinates (Figure 4). Their calculated frequencies are ∼400 and ∼300 cm^{-1} for the singlet and triplet states and some 20−50 cm^{-1} lower for the quintet states, reflecting the antibonding interaction of the singly occupied $d_{x^2-y^2}$ orbital (Table 4). The remaining three vibrations γ_7, γ_8, and γ_9 are out-of-plane modes. Their frequencies are ∼350, ∼260, and ∼100 cm^{-1} for the singlet and triplet states, which are lower by ∼10, ∼100, and ∼30 cm^{-1} for the quintet states, again reflecting the antibonding $d_{x^2-y^2}$ interaction and the flatter potential surface for out-of-plane displacement. We note that relaxation of D_{4h} symmetry constraints for the triplet state has little effect on the e_u modes or γ_9 but lowers the γ_7 and γ_8 frequencies substantially. The reason for this effect is coordinate mixing between a_{2u} and b_{2u} modes both of which have b_{3u} symmetry in the D_{2h} point group. In the E_g states, Jahn−Teller activity of the in-plane b_{1g} and b_{2b} modes will remove the electronic degeneracy by lowering the symmetry to D_{2h}. Geometry optimization under D_{2h} symmetry constraint leads to one of the Jahn−Teller components of the state. This lowering of symmetry splits the e_u modes into b_{1u} and b_{2u} components (D_{2h}), and the a_{2u} and b_{2u} modes (D_{4h}) both correlate with b_{3u} symmetry (D_{2h}). The calculated frequencies of the b_{2u} modes in the $^3A_{2g}$ state are 50, 234, 662, and 784 cm^{-1}. The second of these lies close enough to an a_{2u} mode (γ_8, 254 cm^{-1}) to mix appreciably with it upon lowering the symmetry to D_{2h}. This results in an additional mode with a large iron-atom displacement in the orbitally degenerate states. The γ_8 vibration is mixed between two close-lying modes: 230 and 276 cm^{-1} in the $^3E_g(A)$ state, 220 and 279 cm^{-1} in the $^3E_g(B)$ state, and 183 and 229 cm^{-1} in the ^5E_g state.

The lowest frequency mode, γ_9, is a "doming" motion of the entire molecule (Figure 3), while in γ_8 and γ_7 the Fe out-of-plane displacement is opposed by distortions of the porphyrin

TABLE 4: Calculated Fundamental Frequencies (cm^{-1}) of Normal Modes Involving Large Motions of the Iron Atom in Various Spin States of Iron(II) Porphine and Their Comparison with Other Metalloporphines

		Fe(II)P					MgP[a]	ZnP[a]	NiP[b]
symmetry	mode	$^1A_{1g}$	$^3A_{2g}$	$^3B_{2g}$	$^5A_{1g}$	$^5B_{2g}$	$^1A_{1g}$	$^1A_{1g}$	$^1A_{1g}$
D_{4h}									
a_{2u}	γ_9	98	96	99	71	63	81	77	106
	γ_8	269	248	281	187	158	237	209	280
	γ_7	346	347	362	343	340	346	344	364
e_u	ν_{53}	298	295	291	250	265	322	220	293
	ν_{50}	413	412	410	392	390	453	383	411
		$^3E_g(A)$		$^3E_g(B)$		^5E_g			
D_{2h}									
b_{3u}		96		94		72			
		230		220		183			
		276		279		229			
b_{2u} [b_{1u}][c]		294 [298]		283 [283]		248 [253]			
		412 [426]		403 [403]		391 [395]			

[a] Reference 14. [b] Reference 51. [c] b_{2u}[b_{1u}] denotes pair of e_u frequencies under D_{2h} symmetry.

TABLE 5: Model Frequency Calculations When Hydrogen Atoms in $C_\beta H$ Groups Were by a Particle with a Mass of 15 (Rigid Methyl Group)

		Fe(II)(OEP)		
symmetry	mode	singlet ($^1A_{1g}$)	triplet ($^3A_{2g}$)	quintet ($^5A_{1g}$)
a_{2u}	γ_9	66	65	50
	γ_8	250	234	177
	γ_7	382	380	372
e_u	ν_{53}	292	290	267
	ν_{52}	177	178	176
	ν_{51}	232	233	217
	ν_{50}	349	343	317

skeleton: the pyrrole rings tilt away from the Fe in γ_8, while γ_7 produces alternative up and down displacements of the C_m and N atoms from the mean porphyrin ring. Most of the Fe out-of-plane motion is carried by γ_8 and γ_9, in which the Fe displacement is nearly the same. In γ_7 the Fe displacement is about a third as large for the singlet and triplet states and is much smaller for the quintet state. We note that Warshel and Lappicirella[53] calculated γ_8 and γ_9 at 153 and 54 cm^{-1} using semiempirical QCFF/PI methods, in reasonable agreement with the present values.

The calculated vibrational frequencies are specific to the porphine skeleton, in which all substituents are hydrogens. Physiological porphyrins all have carbon atoms attached to the pyrrole C_β atoms, and these heavier substituents are expected to affect the frequencies somewhat. To estimate this effect we increased the mass of the C_β-hydrogen atoms to 15 amu, representing methyl substituents. The result (Table 5) is to lower the frequency of γ_9 and ν_{50} significantly and to raise the frequency of γ_7. The γ_8 and ν_{53} frequencies stay nearly the same. The ν_{50} lowering is associated with mixing of the C_β-substituent in-plane bending coordinates, which produce additional modes, ν_{51} and ν_{52}, at ~220 and ~170 cm^{-1}. As a result of this mixing, ν_{50} no longer has much iron motion, which is now concentrated in ν_{53}. We note also that the heavy substituents increase the amplitude of the Fe out-of-plane motion in the γ_8 and the γ_9 modes by about 50%.

5. Summary

This is the first density functional calculation of the optimized geometries and force fields of the low-lying spin states of the four-coordinated iron(II)−porphine complex. These calculations, which included nonlocal corrections to the exchange and correlation potential, identify the lowest triplet state of the complex as that with the $^3A_{2g}$ symmetry, the same as predicted by fixed geometry HF calculations,[28,30] among the triplet states. However, in contrast to those calculations, this triplet state is predicted also to be the ground state of the complex (HF calculations strongly underestimate energies of the quintet states owing to the neglect of electronic correlations). Previous density functional calculations[33,34] which suggested the $^3E_g(A)$ state for the ground state of the complex, did not include nonlocal corrections or geometry optimization. We have demonstrated that both gradient corrections and geometry relaxation significantly contribute to the ordering of the spin states in the Fe(II)P complex. An increase of the porphine core size in the quintet states lowers the energies of these states. The calculated core sizes are in excellent agreement with experimental values for six-coordinated Fe(II) porphines establishing the $d_{x^2-y^2}$ occupancy as the main determinant of core size. The calculated core size is the same for intermediate- and low-spin states, but the experimental value is smaller for intermediate-spin Fe(II)-TPP because of ruffling of the porphine ring.

The calculations of the vibrational frequencies and normal modes in the low-lying iron spin states of the complex indicate that there are only five modes carrying large amplitude motions of the iron atom. Three of these are out-of-plane modes of a_{2u} symmetry, of which the mode of the lowest frequency (γ_9) is the doming motion of the complex. The calculated frequency is close to that observed in coherent reaction dynamics in heme proteins.[50] The frequency of this motion is lower in high-spin than in low- or intermediate-spin states of the complex and is sensitive to heavy group substitution on the periphery of the porphine ring. The predicted high-spin frequency is 71 cm^{-1} (or 50 cm^{-1} for mass 15 substituents), not far from the 75 cm^{-1} observed in the coherent reaction dynamics of myoglobin.

Identification of modes with large-amplitude motion of the iron atom as low-frequency out-of-plane a_{2u} modes indicates that the iron atom motion detected in Mössbauer experiments is mostly one-dimensional, acting as a switch between the planar and domed structures. Our calculations confirm the existence of a crossing between states of intermediate- and high-spin multiplicity at domed configurations of the complex. Such a crossing has been previously suggested to explain the observed highly anharmonic motion of the iron atom.[4] In that study the frequency of the doming motion in the ground state was predicted to be around 50 cm^{-1}, and ca. 35 cm^{-1} lower in the upper state involved in the crossing. The present results agree qualitatively with those conclusions. We are now in the process

of extending the calculations to include five- and six-coordinated heme complexes.

Acknowledgment. We thank Prof. M. Parrinello (Stuttgart) for sending us preprints prior to publication and Dr. C. Rovira (Stuttgart) for providing us details about the MDCP calcualtions. Issued as NRCC No. 40860. This work was supported by NIH Grant GM 33576 from the National of Research Medical Science (to T.G.S.).

References and Notes

(1) *Iron Porphyrins*; Lever, A. B., Gray, H. B., Eds.; Physical Bioinorganic Chemistry Series; Addison-Wesley: Reading, MA, 1983; Vols. 1−3.

(2) (a) Scheidt, W. R.; Reed, C. A. *Chem. Rev.* **1981**, *81*, 543. (b) Momenteau, M.; Reed, C. A. *Chem. Rev.* **1994**, *94*, 659.

(3) (a) Parak, F.; Knapp, E. W.; Kucheida, D. *J. Mol. Biol.* **1982**, *161*, 177. (b) Knapp, E. W.; Fischer, S. E.; Parak, F. *J. Phys. Chem.* **1982**, *86*, 5042. (c) Parak, F.; Knapp, E. W. *Proc. Natl. Acad. Sci. U.S.A.* **1984**, *81*, 7088. (d) Nadler, W.; Brunger, A. T.; Schulten, K.; Karplus, K. *Proc. Natl. Acad. Sci. U.S.A.* **1987**, *84*, 7933. (e) Parak, F.; Heidemeier, J.; Nienhaus, G. U. *Hyperfine Interact.* **1988**, *40*, 147.

(4) Li, X. Y.; Zgierski M. Z. *Chem. Phys. Lett.* **1992**, *188*, 16.

(5) Frauenfelder, H.; Parak, F.; Young, R. D. *Annu. Rev. Biophys. Chem.* **1988**, *17*, 451 and references therein.

(6) Collman, J. P.; Hoard, J. L.; Kim, N.; Lang, G.; Reed, C. A. *J. Am. Chem. Soc.* **1975**, *97*, 2676.

(7) Goff, H.; La Mar, G. N.; Reed, C. A., *J. Am. Chem. Soc.* **1977**, *99*, 3641.

(8) Lang, G.; Spartalian, K.; Reed, C. A.; Collman, J. P. *J. Chem. Phys.* **1978**, *69*, 5424.

(9) Dolphin, D.; Sams, J.; Tsin, T. B.; Wong, K. L. *J. Am. Chem. Soc.* **1976**, *98*, 6970.

(10) Kitagawa, T.; Teraoka, J. *Chem. Phys. Lett.* **1979**, *63*, 443.

(11) Almlöf, J.; Fischer, T. H.; Gassman, P. G.; Ghosh, A.; Häser, M. *J. Phys. Chem.* **1993**, *97*, 10964.

(12) Piqueras, M. C.; Rohlfing, C. M. *J. Mol. Struct.: THEOCHEM*, **1996**, *338*, 293.

(13) (a) Kozlowski, P. M.; Zgierski, M. Z.; Pulay, P. *Chem. Phys. Lett.* **1995**, *247*, 379. (b) Kozlowski, P. M.; Jarzęcki, A. A.; Pulay, P. *J. Phys. Chem.*, **1996** , *100*, 7007. (c) Kozlowski, P. M.; Jarzęcki, A. A.; Pulay, P.; Li, X., Y.; Zgierski, M. Z. *J. Phys. Chem.* **1996**, *100*, 13985.

(14) Jarzęcki, A. A.; Kozlowski, P. M.; Pulay, P.; Ye, B. H.; Li, X. Y. *Spectrochim. Acta* **1997**, *A53*, 1195.

(15) Baker, J.; Jarzęcki, A. A.; Kozlowski, P. M.; Pulay, P. *Theor. Chim. Acta* **1997**, *97*, 59.

(16) Becke, A. D. *J. Chem. Phys.* **1993**, *98*, 5648.

(17) Lee, C.; Yang, W.; Parr, R. G. *Phys. Rev.* **1988**, *B 37*, 785.

(18) Frisch, M. J.; Trucks, G. W.; Schlegel, H. B.; Gill, P. M. W.; Johnson, B. G.; Robb, M. A.; Chesseman, J. R.; Keith, T. A.; Petersson, G. A.; Montgomery, J. A.; Raghavachari, K.; Al-Laham, M. A.; Zakrzewski, V. G.; Ortiz, J. V.; Foresman, J. B.; Cioslowski, J.; Stefanov, B. B.; Nanayakkara, A.; Challacombe, M.; Peng, C. Y.; Ayala, P. Y.; Chen, W.; Wong, M. W.; Andres, J. L.; Replogle, E. S.; Gomperts, R.; Marin, R. L.; Fox, D. J.; Binkley, J. S.; Defrees, D. J.; Baker, J.; Stewart, J. P.; Head-Gordon, M.; Gonzalez C.; Pople, J. A. *Gaussian 94*; Gaussian, Inc.: Pittsburgh, PA, 1995.

(19) Schäfer, A.; Horn, H.; Ahlrichs, R. *J. Chem. Phys.* **1992**, *97*, 2571.

(20) Baerends, E. J.; Ellis, D. E.; Ros, P. *Chem. Phys.* **1973**, *2*, 41.

(21) Ravenek, W. In *Algorithms and Applications on Vector and Parallel Computers*; te Riele, H. J. J., Dekker, Th. J., van de Vorst, H. A., Eds.; Elsevier: Amsterdam, 1987. Boerrigter, P. M.; te Velde, G.; Baerends, E., J. *Int. J. Quantum Chem.* **1988**, *33*, 87. te Velde, G.; Baerends, E. J. *J. Comput. Phys.* **1992**, *99*, 84.

(22) Fan, L.; Ziegler, T. *J. Chem. Phys.* **1991**, *94*, 6057. Fan, L.; Ziegler, T. *J. Chem. Phys.* **1991**, *95*, 7401. Fan, L.; Versluis, L.; Ziegler, T.; Baerends, E. J.; Ravenek, W. *Int. J. Quantum Chem.* **1988**, *S22*, 173. Fan, L.; Ziegler, T. *J. Chem. Phys.* **1992**, *96*, 6937, 9005.

(23) Snijders, G. J.; Baerends, E. J.; Vernooijs, P. *At. Nucl. Data Tables* **1982**, *26*, 483. Vernooijs, P.; Snijders, G. J.; Baerends, E. J. *Slater Type Basis Functions for the Whole Periodic System*; Internal report; Free University of Amsterdam: The Netherlands, 1981.

(24) Krijn, J.; Baerends, E. J. *Fit functions in the HFS-method*; Internal Report (in Dutch); Free University of Amsterdam: The Netherlands, 1984.

(25) Vosko, S. H.; Wilk, L.; Nusair, M. *Can. J. Phys.* **1980**, *58*, 1200.

(26) Becke, A. D. *Phys. Rev.* **1988**, *A38*, 2398. Perdew, J. P. *Phys. Rev.* **1986**, *B33*, 8822; *B34*, 7046.

(27) Kashiwagi, H.; Obara, S. *Int. J. Quantum Chem.* **1981**, *20*, 843.

(28) Obara, S.; Kashiwagi, H. *J. Chem. Phys.* **1982**, *77*, 3155.

(29) Sontum S. F.; Case, D. A.; Karplus, M. *J. Chem. Phys.* **1983**, *79*, 2881.

(30) Rawlings, D. C.; Gouterman, M.; Davidson, E. R.; Feller, D. *Int. J. Quantum Chem.* **1985**, *28*, 773.

(31) Rohmer, M. M. *Chem. Phys. Lett.* **1985**, *116*, 44.

(32) Edwards, W. D.; Weiner, B.; Zerner M. C. *J. Am. Chem. Soc.* **1986**, *108*, 2196.

(33) Delley, B. *Physica B* **1991**, *172*, 185. Delley, B. *Density Functional Methods in Chemistry*; Labanowski, J. K., Andzelm J. W., Eds.; Springer-Verlag: New York, 1991; Chapter 7.

(34) Matsuzawa, N.; Ata, M.; Dixon, D. A. *J. Phys. Chem.* **1996**, *100*, 13985.

(35) (a) Rovira, C.; Ballone P.; Parrinello, M. *Chem. Phys. Lett.* **1997**, *271*, 247. (b) Rovira, C.; Kunc, K.; Hutter, J.; Ballone, P.; Parrinello, M. *J. Phys. Chem. A* **1997** *101*, 8914.

(36) The spatial symmetry of the orbitals in the molecular dynamics method of Carr and Parrinello was not controlled. On the basis of the occupation of iron d orbitals, we assigned $^3A_{2g}$ symmetry to lowest triplet and $^5A_{1g}$ to lowest quintet and left the singlet unassiged (C. Rovira, pravite communication).

(37) Radonovich, L.; Bloom, A.; Hoard, J. *J. Am. Chem. Soc.* **1972**, *94*, 2073.

(38) Reed, C. A.; Mashiko, T.; Scheidt, W. R.; Spartalian, K.; Lang, G. *J. Am. Chem. Soc.* **1980**, *102*, 2073.

(39) (a) Cullen, D. L.; Meyer, E. F., Jr. *J. Am. Chem. Soc.* **1974** *41A*, 1443. (b) Brennan, T. D.; Scheidt, W. R.; Shelnutt, J. A. *J. Am. Chem. Soc.* **1988**, *110*, 3919. (c) Meyer, E. F., Jr. *Acta Crystallogr.* **1972**, *B28*, 2162.

(40) Hoard, J. L. *Science* **1971**, *174*, 1295.

(41) Cotton, F. A.; Wilkinson, G. *Advanced Inorganic Chemistry*; Wiley: New York, 1972; p 871.

(42) Hoard, J. L. *Porphyrins and Metalloporphyrins*; Smith, K. M., Ed.; Elsevier: Amsterdam, 1975; pp 317−380.

(43) Olafson, B. D.; Goddard, W. A. III. *Proc. Natl. Acad. Sci. U.S.A.* **1977**, *74*, 1315.

(44) Dedieu, A.; Rohmer, M. M.; Veillard, A. *Adv. Quantum Chem.* **1982**, *16*, 43.

(45) Rohmer, M.-M.; Dedieu, A.; Veillard, A. *Chem. Phys.* **1983**, *77*, 449.

(46) Fermi, G.; Perutz, M. F.; Shaana, B.; Fourne, R., *J. Mol. Biol.* **1984**, *111*, 5509.

(47) Yang, F.; Phillips, G. N., Jr. *J. Mol. Biol.* **1996**, *256*, 762.

(48) Jameson, G. B.; Molinaro, F. S.; Ibers, J. A.; Colleman, J. P.; Brauman, J. I.; Rose, E.; Suslick, K. S. *J. Am. Chem. Soc.* **1980**, *102*, 3224.

(49) Loew, G. Reference 1, Vol. 1, Chapter 1.

(50) Zhu, L.; Sage, T.; Champion, P. M. *Science* **1994**, *226*, 629.

(51) Kozlowski P.; Zgierski M. Z.; et al. Unpublished work.

(52) Spiro, T. G.; Li, X. Y. In *Biological Applications of Raman Spectroscopy*; Spiro, T. G., Ed.; Wiley-Interscience, New York 1988; p 1.

(53) Warshel, A.; Lappicirella, A. *J. Am. Chem. Soc.* **1981**, *103*, 4664.